NACA RM L53J23

NACA

RESEARCH MEMORANDUM

PRELIMINARY DRAG MEASUREMENTS OF THE CONSOLIDATED VULTEE XF-92A DELTA-WING AIRPLANE IN FLIGHT TESTS TO A MACH NUMBER OF 1.01

By Donald R. Bellman and Thomas R. Sisk

Langley Aeronautical Laboratory
Langley Field, Va.

NATIONAL ADVISORY COMMITTEE
FOR AERONAUTICS

WASHINGTON

January 4, 1954
Declassified January 10, 1957

NATIONAL ADVISORY COMMITTEE FOR AERONAUTICS

RESEARCH MEMORANDUM

PRELIMINARY DRAG MEASUREMENTS OF THE CONSOLIDATED VULTEE XF-92A DELTA-WING AIRPLANE IN FLIGHT

TESTS TO A MACH NUMBER OF 1.01

By Donald R. Bellman and Thomas R. Sisk

SUMMARY

Preliminary drag data were obtained for the XF-92A delta-wing airplane during U. S. Air Force demonstration tests of the airplane after it had been modified to use the J33-A-29 turbojet engine. Drag data were obtained over a lift-coefficient range for Mach numbers from 0.63 to 0.90 and for a lift coefficient of 0.08 to a Mach number of 1.01. The lift-curve slopes when corrected to zero elevator deflection varied from 2.6 radian^{-1} at a Mach number of 0.63 to 2.9 radian^{-1} at a Mach number of 0.94. For a lift coefficient of 0.08 the drag rise occurred at a Mach number of 0.91. Below the drag rise the drag coefficient was approximately constant at a value of 0.009. Between Mach numbers of 0.99 and 1.01 the drag coefficient was approximately constant at a value of 0.040. The slope dC_D/dC_L^2 (where C_D is drag coefficient and C_L, lift coefficient) varies with lift over a large portion of the lift range.

INTRODUCTION

The XF-92A airplane was constructed by Consolidated Vultee Aircraft Corporation to provide research information on the flight characteristics of the delta-wing configuration at subsonic speeds. The results of demonstration flight tests conducted by the manufacturer were reported in reference 1 and the results of U. S. Air Force performance and stability tests were reported in reference 2. From these tests, drag data to a Mach number of 0.925 were reported.

At the request of the Air Force, the XF-92A power plant, an Allison J33-A-23 turbojet engine, was replaced by the more powerful J33-A-29 model which is equipped with an afterburner. This modification was made as a result of the increased interest in the delta-wing configuration as a supersonic airplane.

This paper presents drag data obtained during the Air Force demonstration and performance tests of the new power plant. The NACA High-Speed Flight Research Station supplied engineering, instrumentation, and operational assistance for the program. The tests were made in the period from July 1951 through February 1953 at the Air Force Flight Test Center at Edwards, Calif.

SYMBOLS

A	tail-pipe exit area, sq ft
a_X	measured longitudinal acceleration, g units
C_D	drag coefficient
C_{D_0}	zero-lift drag coefficient
C_f	thrust coefficient
C_L	lift coefficient
C_{L_α}	lift-curve slope, radians^{-1}
C_N	normal-force coefficient
C_X	longitudinal-force coefficient
dC_D/dC_L^2	drag-due-to-lift factor
F_j	jet thrust, lb
F_n	net thrust, lb
g	acceleration due to gravity, ft/sec^2
M	Mach number
M.A.C.	mean aerodynamic chord, ft
N	engine speed, rpm
n	normal acceleration, g units

p	atmospheric pressure, lb/sq ft
p_6	static pressure at tail-pipe exit, lb/sq ft
p_{t_6}	total pressure at tail-pipe exit, lb/sq ft
q	dynamic pressure, lb/sq ft
S	wing area, sq ft
T	atmospheric temperature, $^{\circ}R$
T_t	inlet air total temperature, $^{\circ}R$
W	airplane weight, lb
w	engine air flow, lb/sec
α	angle of attack, deg
γ	ratio of specific heats
δ_c	altitude normalizing factor, $\frac{p(1 + 0.2M^2)^{3.5}}{2116}$
δ_e	elevator deflection, $\frac{\delta_{e_{Left}} + \delta_{e_{Right}}}{2}$, deg
θ_c	temperature normalizing factor, $\frac{T(1 + 0.2M^2)}{518.4}$

AIRPLANE

The Consolidated Vultee XF-92A airplane is a single-place 60° delta-wing airplane powered by a turbojet engine and afterburner. The wing has a streamwise thickness ratio of 6.5 percent. The vertical stabilizer is also swept back 60° and there is no horizontal stabilizer. The airplane has no leading- or trailing-edge slats or flaps, no dive brakes, and no trim tabs. Both elevator and rudder trim are accomplished by means of electric actuators which re-position the control linkage and thereby move the entire control surfaces. The turbojet engine produces a test stand thrust of 5,600 pounds at sea level, which is increased to

7,500 pounds by means of the afterburner. However, when the engine is installed in the airplane, the thrust is reduced to about 4,500 pounds which the afterburner increases to 5,700 pounds. Part of the reduction in thrust is caused by the fact that the ducts and plenum chamber were designed for a smaller engine. A two-position eyelid on the tail pipe is used to maintain proper pressures with the afterburner on and off.

Table I lists the physical characteristics and figure 1 shows a three-view drawing of the airplane. Photographs of the airplane are presented in figure 2.

INSTRUMENTATION

The airplane was equipped with standard NACA recording instruments for measuring airspeed, pressure altitude, angle of attack, accelerations, and the various pressures needed for thrust calculation. The airspeed head, angle-of-attack vane, and angle-of-yaw vane are mounted on a nose boom projecting from the air inlet opening. The tip of the airspeed head is located 64.9 inches ahead of the duct inlet. A type A-6 total head tube, described in reference 3, was used and it requires no correction between angles of attack of -14° and 34°. The angle-of-attack vane was located on a post projecting from the side of the boom so that the blade was 7.5 inches to the left of the boom and 36 inches ahead of the duct inlet. A shielded resistance-type thermometer used to obtain the free-air total temperature was attached to the boom 22 inches in front of the duct inlet.

The total pressure of the tail pipe was measured by two probes projecting around the lip of the eyelid and connected to a common recording manometer cell. Each probe consisted of two concentric tubes and cooling air from the compressor bleed was passed through the annulus. Compressor inlet conditions were measured by four rakes mounted 90° apart in the plenum chamber. Each rake has a total pressure tube and a static pressure tube. Like components of all four rakes were connected to a single recorder.

THRUST AND DRAG CALCULATIONS

The jet thrust, which is the force resulting from the total momentum of the gas leaving the tail pipe, was calculated using the tail-pipe total pressure. The exact formula used depended on whether the velocity of exhaust gas at the nozzle exit was subsonic or sonic. The critical pressure ratio for exhaust gas was assumed to be 1.851. If the ratio of the

tail-pipe total pressure to atmospheric pressure was equal to or greater than this figure, sonic velocity was assumed; otherwise subsonic velocity was assumed. The general equation for calculating jet thrust is

$$F_j = C_f A \left\{ p_6 \left(\frac{2\gamma}{\gamma - 1} \right) \left[\left(\frac{p_{t_6}}{p_6} \right)^{\frac{\gamma-1}{\gamma}} - 1 \right] + p_6 - p \right\}$$

For subsonic tail-pipe velocities the tail-pipe static pressure p_6 was assumed equal to the atmospheric pressure p, which reduced the formula to

$$F_j = C_f A p \left(\frac{2\gamma}{\gamma - 1} \right) \left[\left(\frac{p_{t_6}}{p} \right)^{\frac{\gamma-1}{\gamma}} - 1 \right]$$

For sonic tail-pipe velocities the tail-pipe static pressure p_6 was assumed equal to the tail-pipe total pressure divided by the critical pressure ratio $p_{t_6}/1.851$ and the formula then becomes

$$F_j = C_f A \left\{ \frac{p_{t_6}}{1.851} \left(\frac{2\gamma}{\gamma - 1} \right) \left[(1.851)^{\frac{\gamma-1}{\gamma}} - 1 \right] + \frac{p_{t_6}}{1.851} - p \right\}$$

This equation reduces to

$$F_j = C_f A \left(1.259 p_{t_6} - p \right)$$

The thrust coefficient C_f was taken to be the ratio of true thrust as measured on the Air Force thrust stand at Edwards Air Force Base to the jet thrust as determined from the tail-pipe pressure measurements and ambient pressure and temperature. Figure 3 shows the variation of C_f with the pressure ratio p_{t_6}/p. In all cases γ was assumed to be 1.33 for exhaust gas.

The ram drag, which is the force resulting from the total momentum of the air entering the engine, was obtained from the product of the true airplane velocity and the air flow into the engine. The true airplane velocity was calculated from the true Mach number and the free-air static temperature, which was obtained from the free-air total temperature by means of the following relationship

$$T = \frac{T_t}{1 + 0.198M^2}$$

The air flow through the engine was measured by considering the engine to be a constant volume pump; in other words, it was assumed that the plot of normalized air flow $w\sqrt{\theta_c}/\delta_c$ against normalized engine speed $N/\sqrt{\theta_c}$ was valid for all Mach numbers, altitudes, and engine speeds. The pressure normalizing factor was based on the total pressure in the plenum chamber just ahead of the engine and the temperature normalizing factor was based on the free-air total temperature as measured on the boom ahead of the inlet duct. The engine air-flow plot shown in figure 4 was based on tests made by the engine manufacturer. The net thrust was taken to be the difference between the jet thrust and the ram drag. The methods of measuring these latter two quantities make the net thrust equal to the change in momentum of the air and fuel passing through the engine and effects of cooling air and compressor bleed air are neglected.

The accelerometer method was used to determine the drag forces and the following equations were used to calculate the lift and drag coefficients:

$$C_N = \frac{nW}{qS}$$

$$C_X = \frac{F_n - Wa_X}{qS}$$

$$C_L = C_N \cos \alpha - C_X \sin \alpha$$

$$C_D = C_X \cos \alpha + C_N \sin \alpha$$

ACCURACY

The airspeed installation was calibrated using the radar-phototheodolite method described in reference 4. The low-speed static pressure calibration needed for the pressure survey in the method was obtained from an Air Force F-86 pacer airplane and checked with pressure surveys obtained by a radiosonde balloon. The calibration method resulted in Mach numbers that are probably accurate to within ±0.01.

Inaccuracies in the angle-of-attack measurements result from the following sources: instrument capabilities, vane floating, boom bending, and upwash. The instrumentation was such that the position of the vane can be measured to within ±0.2°. The only error for which corrections were made was that caused by the inertia loads on the boom. This error amounted to 0.16° per g and was determined by statically loading the boom at intervals to simulate inertia loads up to 7g. No corrections were made for errors caused by vane floating, air loads on the boom, and upwash because there were insufficient data concerning these errors that were applicable to this airplane, and it was not practical during the present program to make the special flights necessary to determine the errors. The relative magnitudes of some of the errors are indicated in reference 5, which shows that the vane-floating error can amount to 0.4° and the upwash due to the boom would cause an error of about 5 percent in angle of attack. Also in reference 5 are data for an F-86 airplane which indicate that at a comparable position ahead of the inlet the effect of upwash due to the wing and fuselage would be of the order of 0.5° for the Mach number and lift ranges involved.

Inaccuracies in thrust result from the fact that thrust calibrations are made on the ground with approximately sea-level pressure and temperature. Consequently, most of the flight data require the use of the extrapolated portions of the thrust-coefficient curve (fig. 3) and the air-flow curve (fig. 4). Furthermore, the entire ground calibration takes place with a subsonic tail-pipe velocity, whereas for the major portion of the flight data the tail-pipe velocity is sonic. There is reason to believe that there is less pressure recovery at the rear face of the compressor than at the forward face; however, the air-flow measurement with which the ram drag is calculated is based on measurements applicable to the forward face. This would cause the air-flow measurements to be high. It is estimated that the thrust values are accurate to within ±200 pounds.

The following accuracies are estimated for the other measurements:

Normal acceleration, g units	±0.05
Longitudinal acceleration, g units	±0.025
Airplane weight, lb	±100
Angle of attack, deg	±1.0

The drag-coefficient values are affected primarily by inaccuracies in angle of attack, thrust, and longitudinal acceleration. The standard deviation of drag coefficient was determined from the method of reference 5 by using the maximum estimated error of the above three quantities. At an altitude of 10,000 feet, as the Mach number varies from 0.63 to 1.0, the uncertainty in drag coefficient will vary from 0.0016 to 0.0006; whereas at an altitude of 40,000 feet the uncertainty will vary from 0.0050 to 0.0023. These figures are for level-flight conditions and the deviation will be slightly greater at higher lift conditions.

TESTS, RESULTS, AND DISCUSSION

The data presented in this paper were taken from six flights flown for the U. S. Air Force demonstration program. The maneuvers consisted of level runs, climbs, high-speed dives, and pull-ups. Test altitude varied from 6,000 to 40,000 feet, and Reynolds number based on the mean aerodynamic chord varied from 25×10^6 to 80×10^6. Data are presented for five approximately constant Mach numbers ranging from 0.63 to 0.94. The data for each curve cover a narrow range of Mach number about the given Mach number, which varied from ± 0.03 at a Mach number of 0.63 to ± 0.005 at a Mach number of 0.94. The data at Mach numbers of 0.63, 0.70, and 0.84 came almost entirely from three low-altitude pull-ups, whereas the data at Mach numbers of 0.90 and 0.94 came primarily from a group of high-speed dives and pull-outs. There were appreciable pitching oscillations during the dives and pull-outs which might account for increased scatter in these data.

Figure 5 shows the variation of lift coefficient with angle of attack for the five Mach numbers varying from 0.63 to 0.94. The figure shows data for trim elevator position and also the same data corrected to zero elevator position. The correction was made by using values of $dC_L/d\delta_e$ obtained from wind-tunnel tests (ref. 6). It can be seen that the elevator position affects both the lift values and the lift-curve slopes. The effect on the lift-curve slope comes primarily from the fact that the trim elevator position is varying more or less uniformly with angle of attack, since the difference in slope for two different, but constant, elevator positions is slight. (See ref. 7.)

The lift-curve slopes obtained from figure 5 are plotted against Mach number in figure 6. The lift-curve slopes for the condition of zero elevator deflection vary from about 2.6 radians^{-1} at a Mach number of 0.63 to about 2.9 radians^{-1} at a Mach number of 0.94 which is about 0.6 radian^{-1} higher than for the data uncorrected for elevator position.

The variation of drag coefficient with Mach number for a lift coefficient of about 0.08 is presented in figure 7. Between Mach numbers of 0.65 and 0.82 the drag coefficient has a value of about 0.0093. If the drag-rise Mach number is defined as the Mach number at which the rate of change of drag coefficient with Mach number becomes 0.10, then for the XF-92A airplane at a lift coefficient of 0.08 the drag rise occurs at a Mach number of about 0.91. The increase in drag coefficient with Mach number ceases at a Mach number of about 0.99 and from this Mach number to a Mach number of 1.01, the test limit, the drag coefficient is approximately constant at a value of 0.040.

Figure 8 shows the drag coefficient plotted against lift coefficient for the same maneuvers as presented in figure 5. The drag data for a Mach number of 0.94 were omitted because of excessive scatter which is to be expected in the region where the drag varies greatly with Mach number. The variation in elevator angle with lift for each Mach number is shown by the table on the figure.

The data of figure 8 are plotted in figure 9 as a function of the square of the lift coefficient. Such plots have been useful for many airplanes, particularly those with straight wings and high aspect ratios, because the slopes of the curves dC_D/dC_L^2 are constant over the normal lift range of the airplane. Figure 9 shows, however, that for the XF-92A airplane the slope dC_D/dC_L^2 is not constant but varies with lift over a large portion of the lift range.

CONCLUSIONS

The following conclusions were drawn from the results of lift and drag data obtained from flight tests of the Consolidated Vultee XF-92A airplane.

1. The lift-curve slopes when corrected to zero elevator deflection vary from 2.6 radians^{-1} at a Mach number of 0.63 to 2.9 radians^{-1} at a Mach of 0.94.

2. For a lift coefficient of 0.08 the drag rise occurred at a Mach number of 0.91. Below the drag rise the drag coefficient was approximately constant at a value of 0.009. Between Mach numbers of 0.99 and 1.01 the drag coefficient was approximately constant at a value of 0.040.

3. The slope dC_D/dC_L^2 varies with lift over a large portion of the lift range.

Langley Aeronautical Laboratory,
National Advisory Committee for Aeronautics,
Langley Field, Va., October 6, 1953.

REFERENCES

1. Anon.: Flight Test Memorandum XF-92A (Model 7002) Airplane. Rep. Nos. F-7002-1, F-7002-2, F-7002-3, F-7002-4, F-7002-5, F-7002-6, Consolidated Vultee Aircraft Corp., 1949.

2. Mapp, Robert, Yeager, Charles E., and Everest, Frank K.: Phase II Flight Tests of the XF-92A Airplane, USAF No. 46-682. Memo. Rep. No. MCRFT-2262, Air Materiel Command, Flight Test Div., U. S. Air Force, Dec. 20, 1949.

3. Gracey, William, Letko, William, and Russell, Walter R.: Wind-Tunnel Investigation of a Number of Total-Pressure Tubes at High Angles of Attack - Subsonic Speeds. NACA TN 2331, 1951. (Supersedes NACA RM L50G19.)

4. Zalovcik, John A.: A Radar Method of Calibrating Airspeed Installations on Airplanes in Maneuvers at High Altitudes and at Transonic and Supersonic Speeds. NACA Rep. 985, 1950. (Supersedes NACA TN 1979.)

5. McFadden, Norman M., Holden, George R., and Ratcliff, Jack W.: Instrumentation and Calibration Technique for Flight Calibration of Angle-of-Attack Systems on Aircraft. NACA RM A52I23, 1952.

6. Lawrence, Leslie F., and Summers, James L.: Wind-Tunnel Investigation of a Tailless Triangular-Wing Fighter Aircraft at Mach Numbers From 0.5 to 1.5. NACA RM A9B16, 1949.

7. Mitcham, Grady L., Crabill, Norman L., and Stevens, Joseph E.: Flight Determination of the Drag and Longitudinal Stability and Control Characteristics of a Rocket-Powered Model of a 60° Delta-Wing Airplane From Mach Numbers of 0.75 to 1.70. NACA RM L51I04, 1951.

TABLE I

PHYSICAL CHARACTERISTICS OF THE XF-92A AIRPLANE

Wing:	
Area, sq ft	425
Span, ft	31.33
Airfoil section	NACA $65_{(06)}$-006.5
Mean aerodynamic chord, ft	18.09
Aspect ratio	2.31
Root chord, ft	27.13
Tip chord	0
Taper ratio	0
Sweepback (leading edge), deg	60
Incidence, deg	0
Dihedral (chord plane), deg	0
Elevons:	
Area (total, both, aft of hinge line) sq ft	76.19
Span (one elevon), ft	13.35
Chord (aft of hinge line, constant except at tip), ft	3.05
Movement, deg	
Elevator:	
Up	15
Down	5
Aileron, total	10
Operation	Hydraulic
Vertical tail:	
Area, sq ft	75.35
Height, above fuselage center line, ft	11.50
Rudder:	
Area, sq ft	15.53
Span, ft	9.22
Travel, deg	±8.5
Operation	Hydraulic
Fuselage:	
Length, ft	42.80
Power plant:	
Engine	Allison J33-A-29 with afterburner
Rating:	
Static thrust at sea level, lb	5600
Static thrust at sea level with afterburner, lb	7500

TABLE I - Concluded

PHYSICAL CHARACTERISTICS OF THE XF-92A AIRPLANE

Weight:	
Gross weight (560 gal fuel), lb	15,560
Empty weight, lb	11,808
Center-of-gravity locations:	
Gross weight (560 gal fuel), percent M.A.C.	25.5
Empty weight, percent M.A.C.	29.2
Moment of inertia in pitch, slug-ft^2	35,000

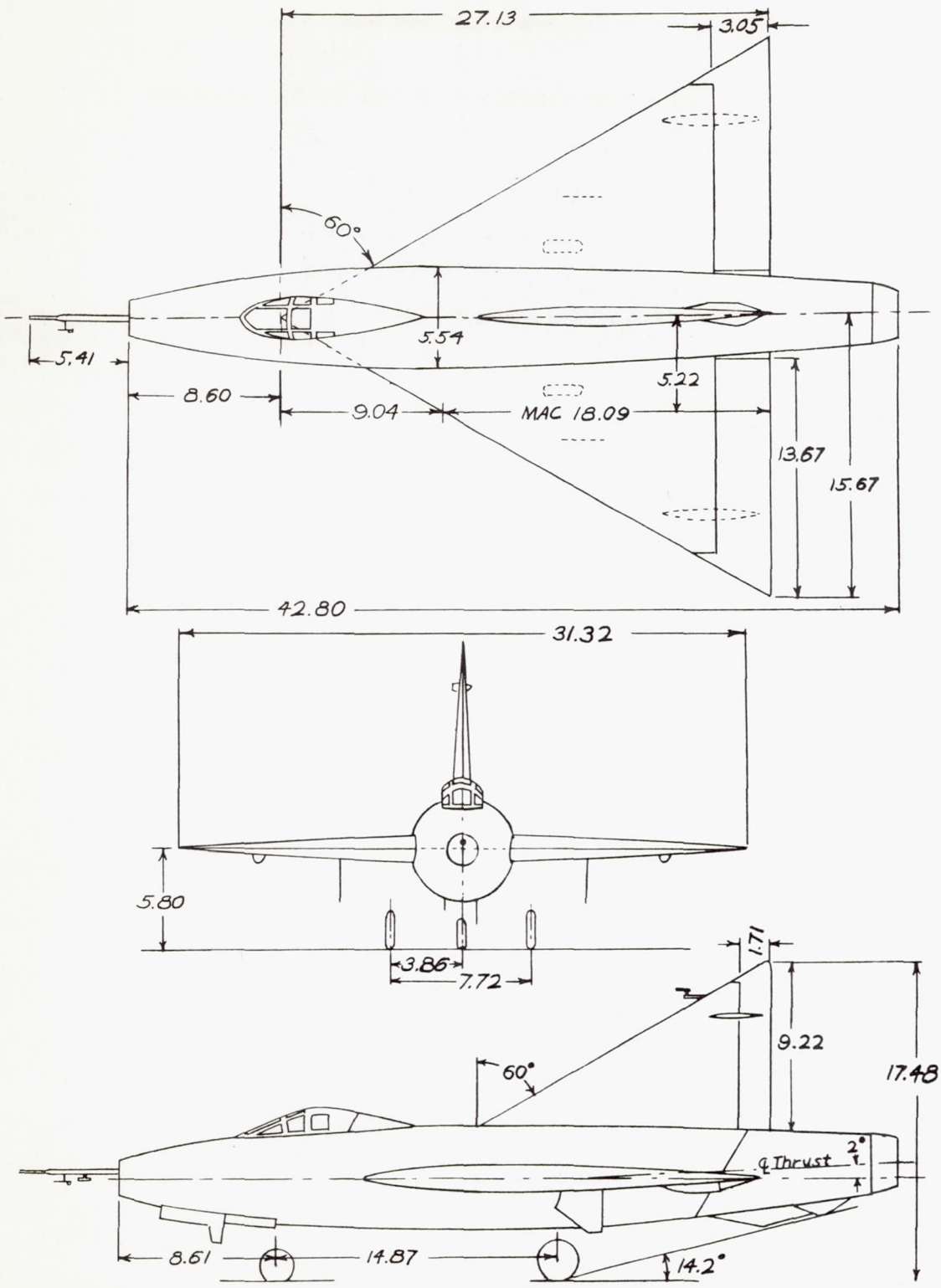

Figure 1.- Three-view drawing of XF-92A airplane. All dimensions are in feet.

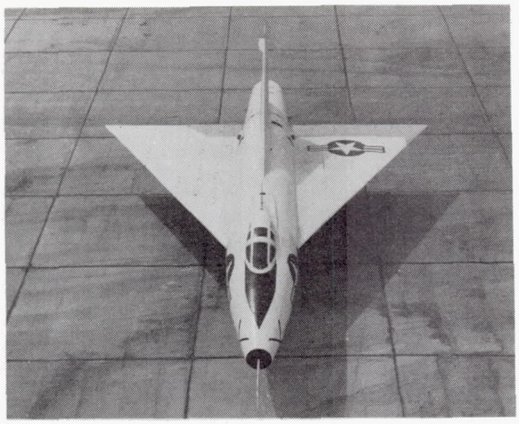

(a) Overhead front view.

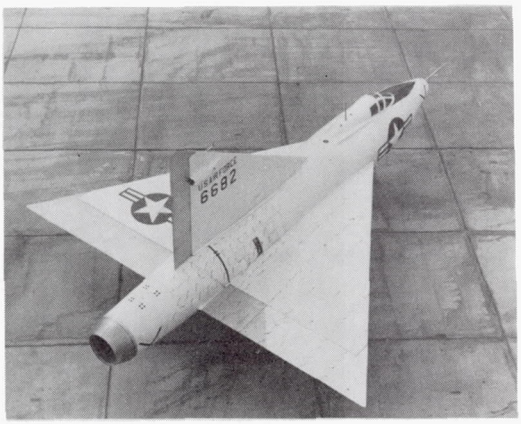

(b) Three-quarter rear view.

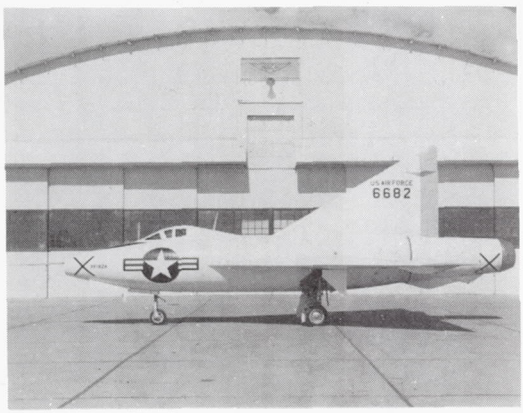

L-81260

(c) Left side view.

Figure 2.- Photographs of XF-92A research airplane.

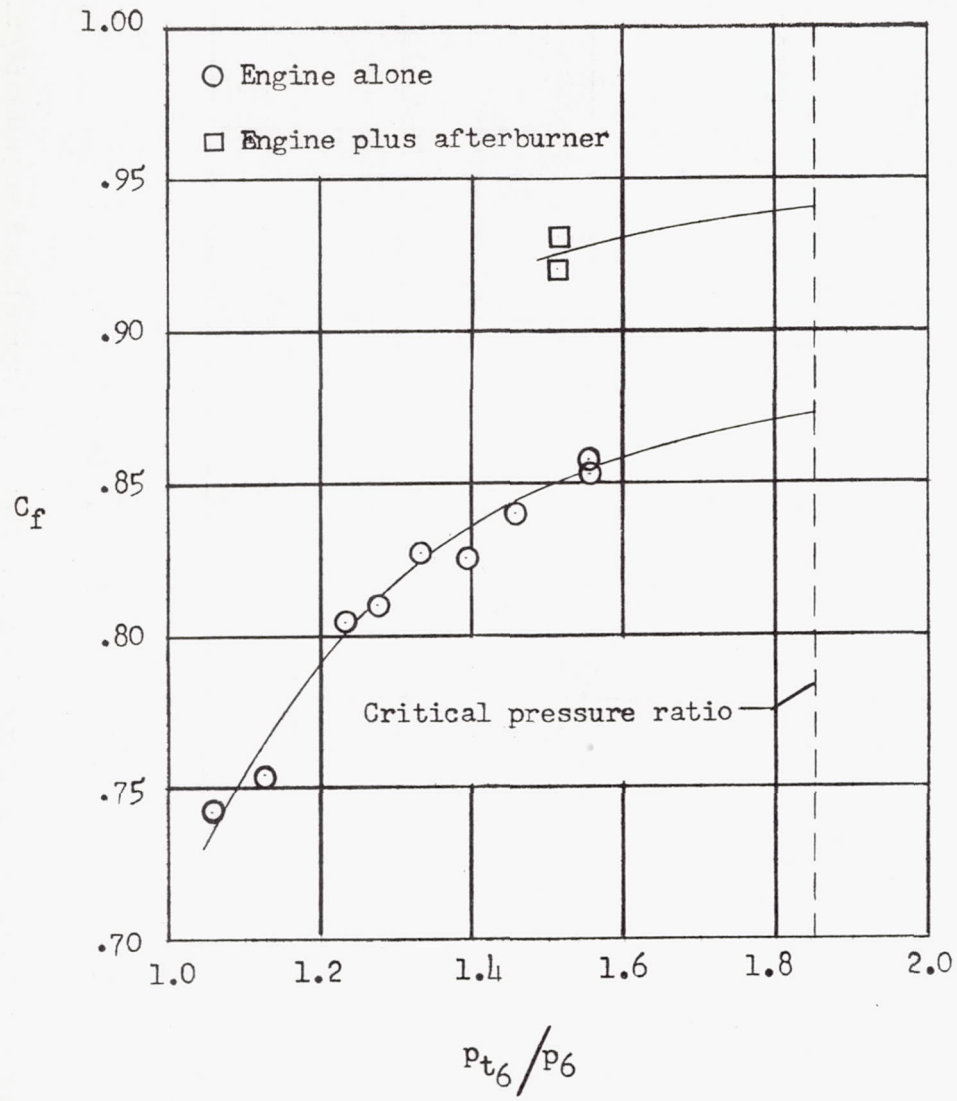

Figure 3.- Variation of thrust coefficient with tailpipe pressure ratio.

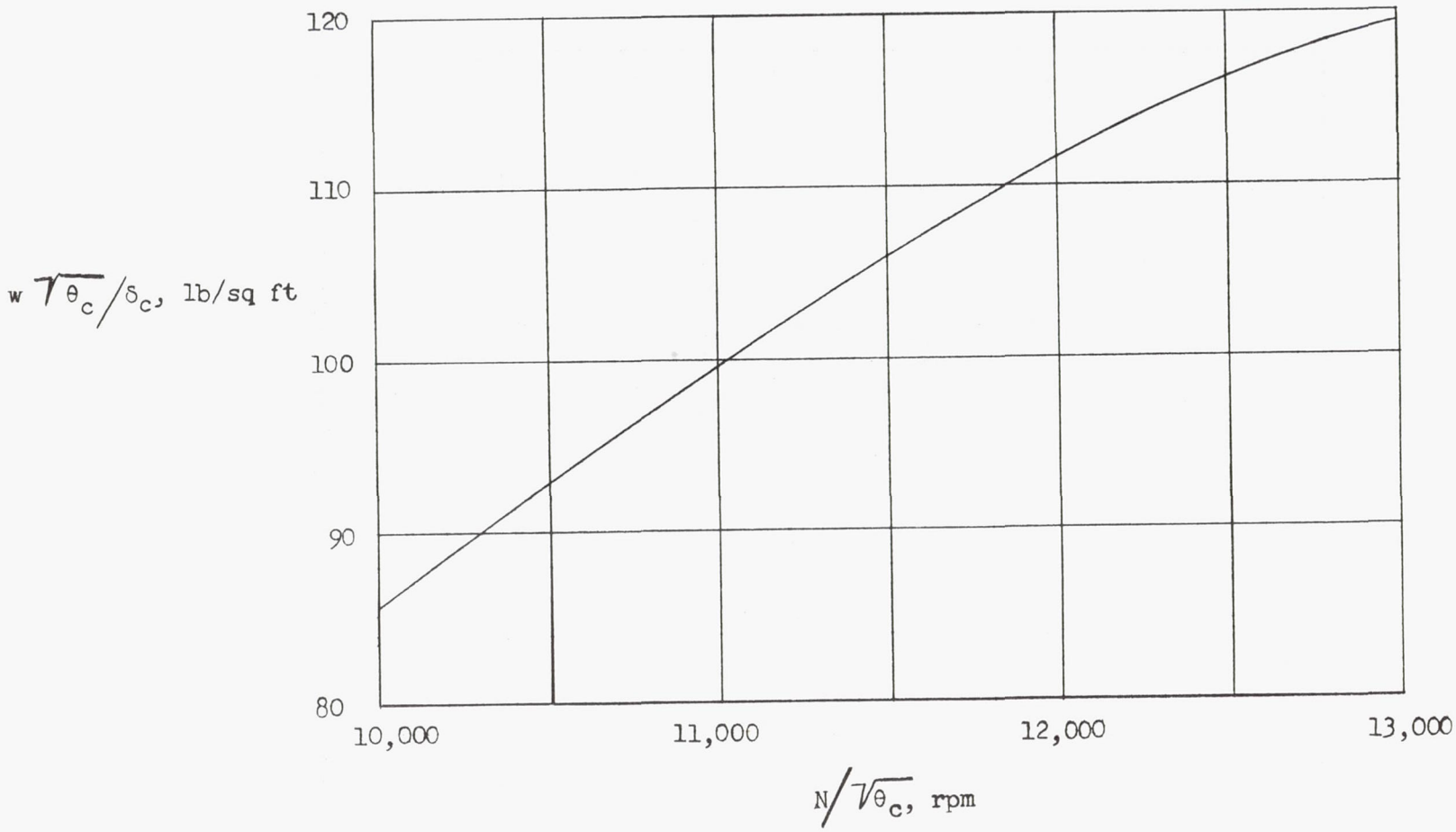

Figure 4.- Variation of normalized air flow with normalized engine speed.

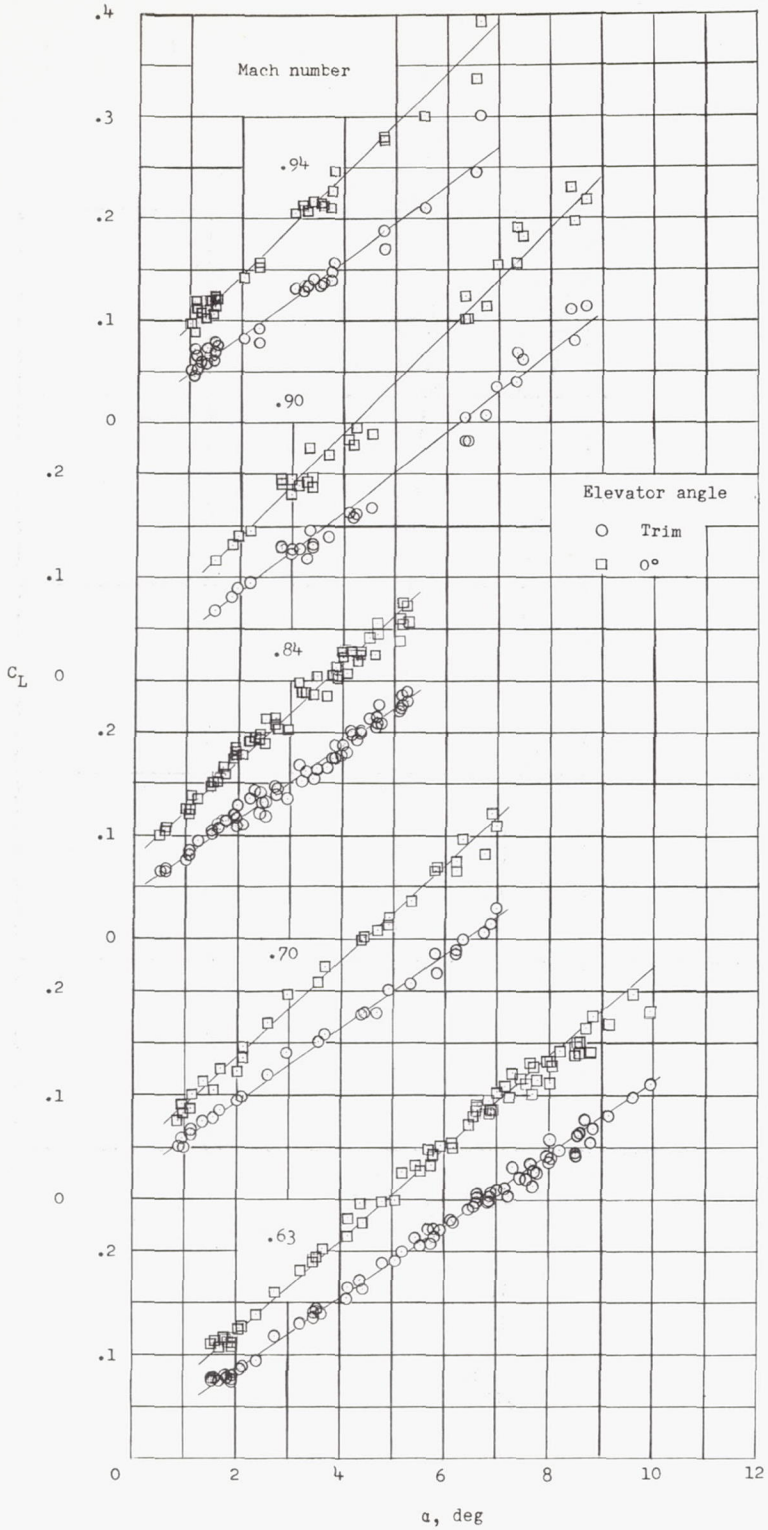

Figure 5.- Variation of lift coefficient with angle of attack for various constant Mach numbers.

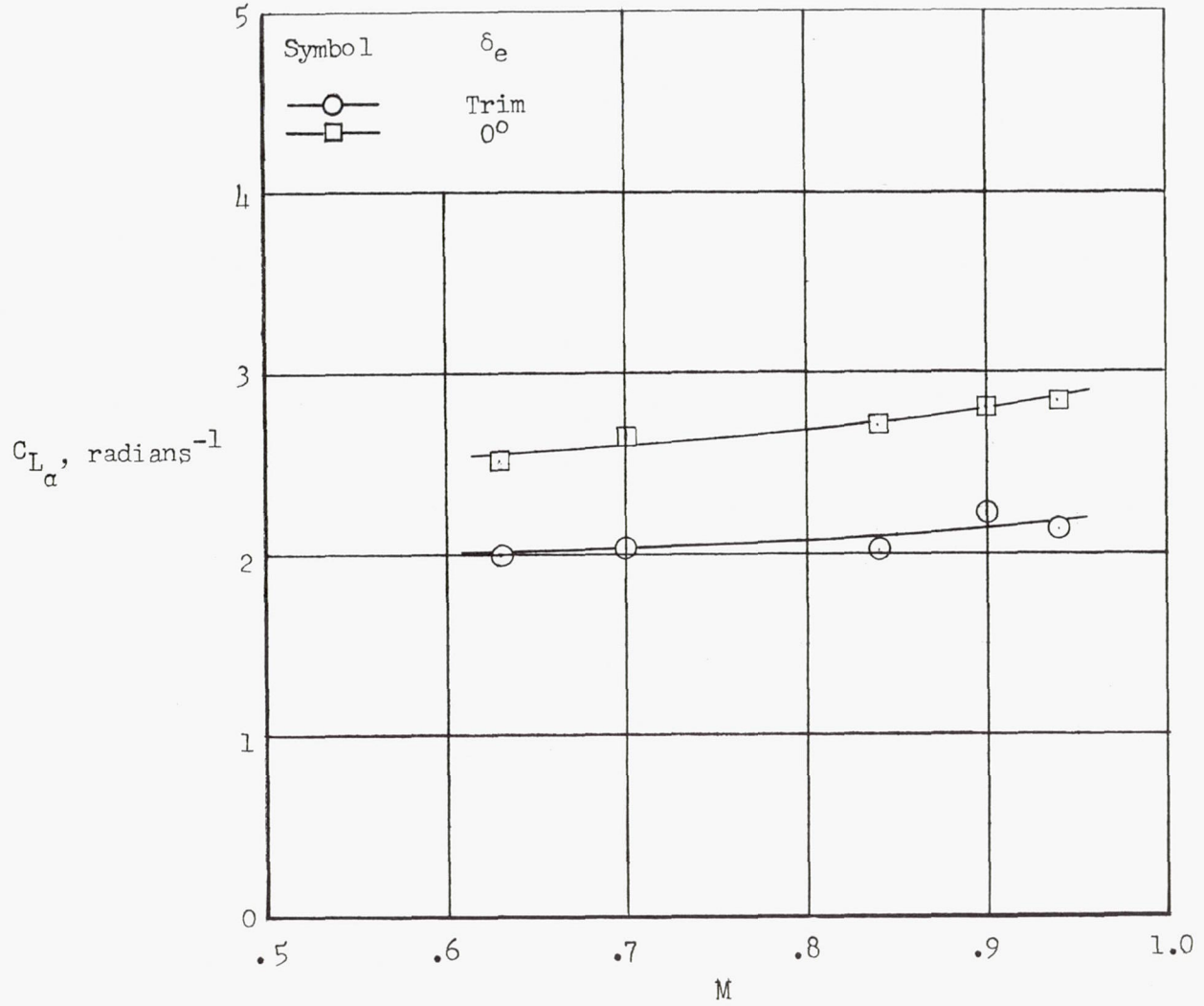

Figure 6.- Variation of lift-curve slopes with Mach number for trimmed flight conditions and for the data corrected to zero elevon deflection.

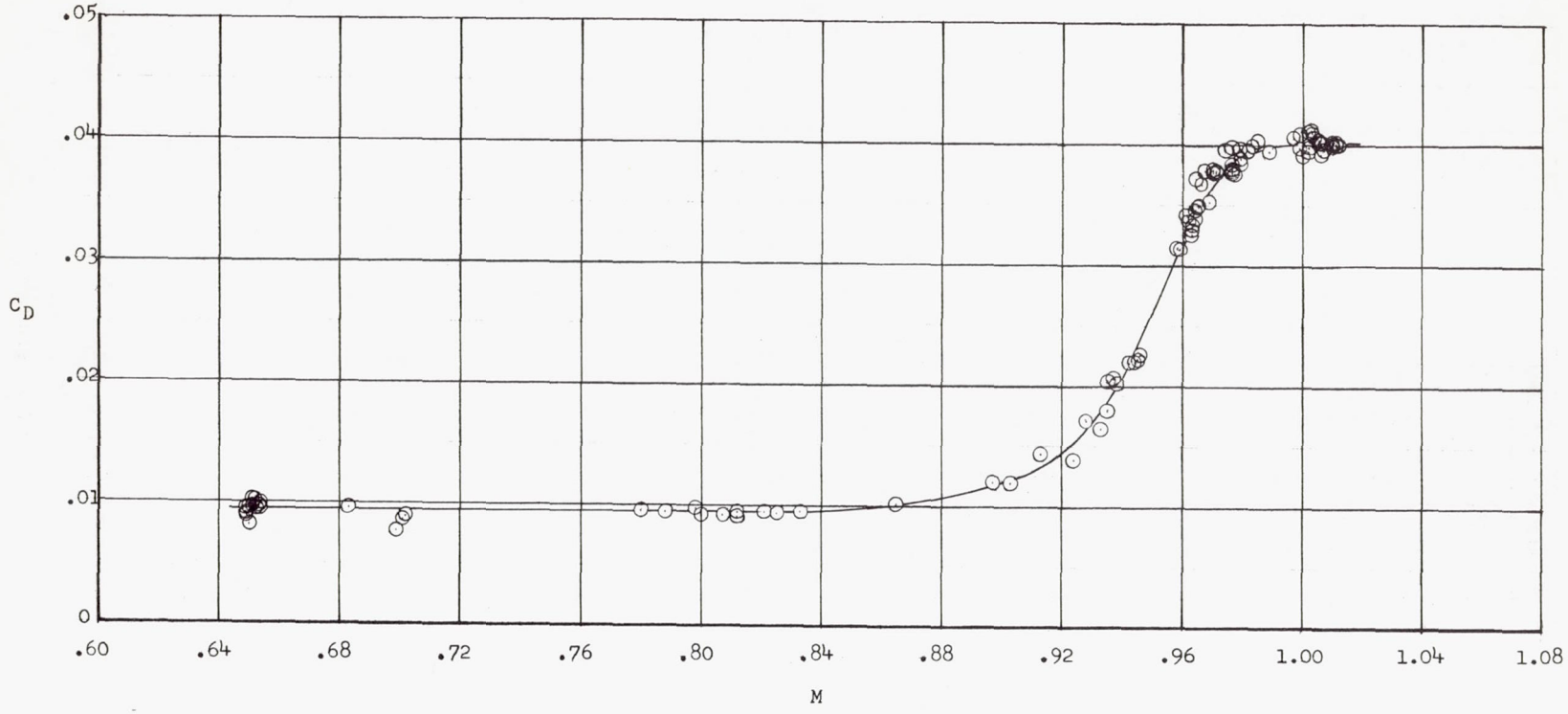

Figure 7.- Variation of drag coefficient with Mach number for a lift coefficient of 0.08.

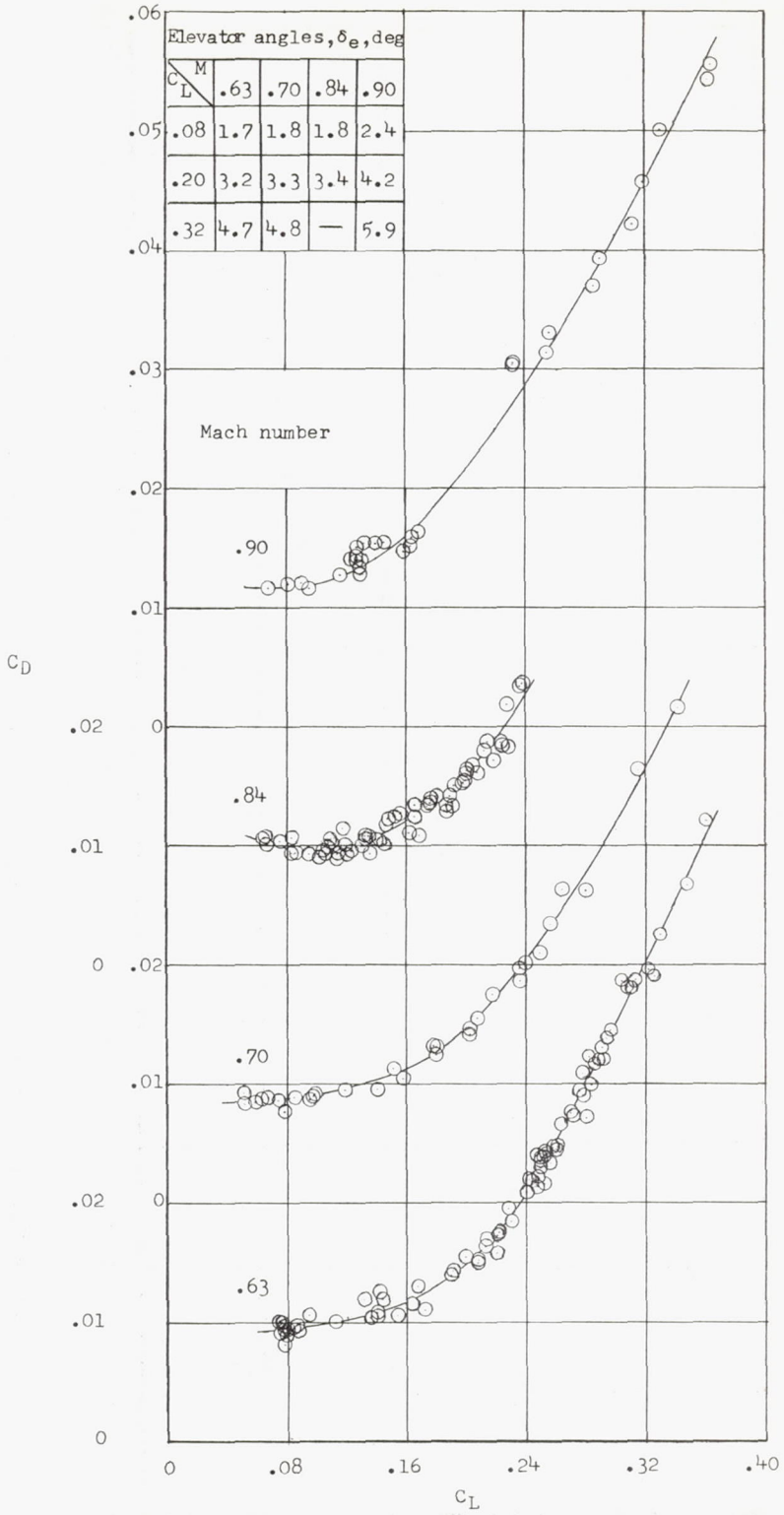

Figure 8.- Variation of drag coefficient with lift coefficient for four Mach numbers.

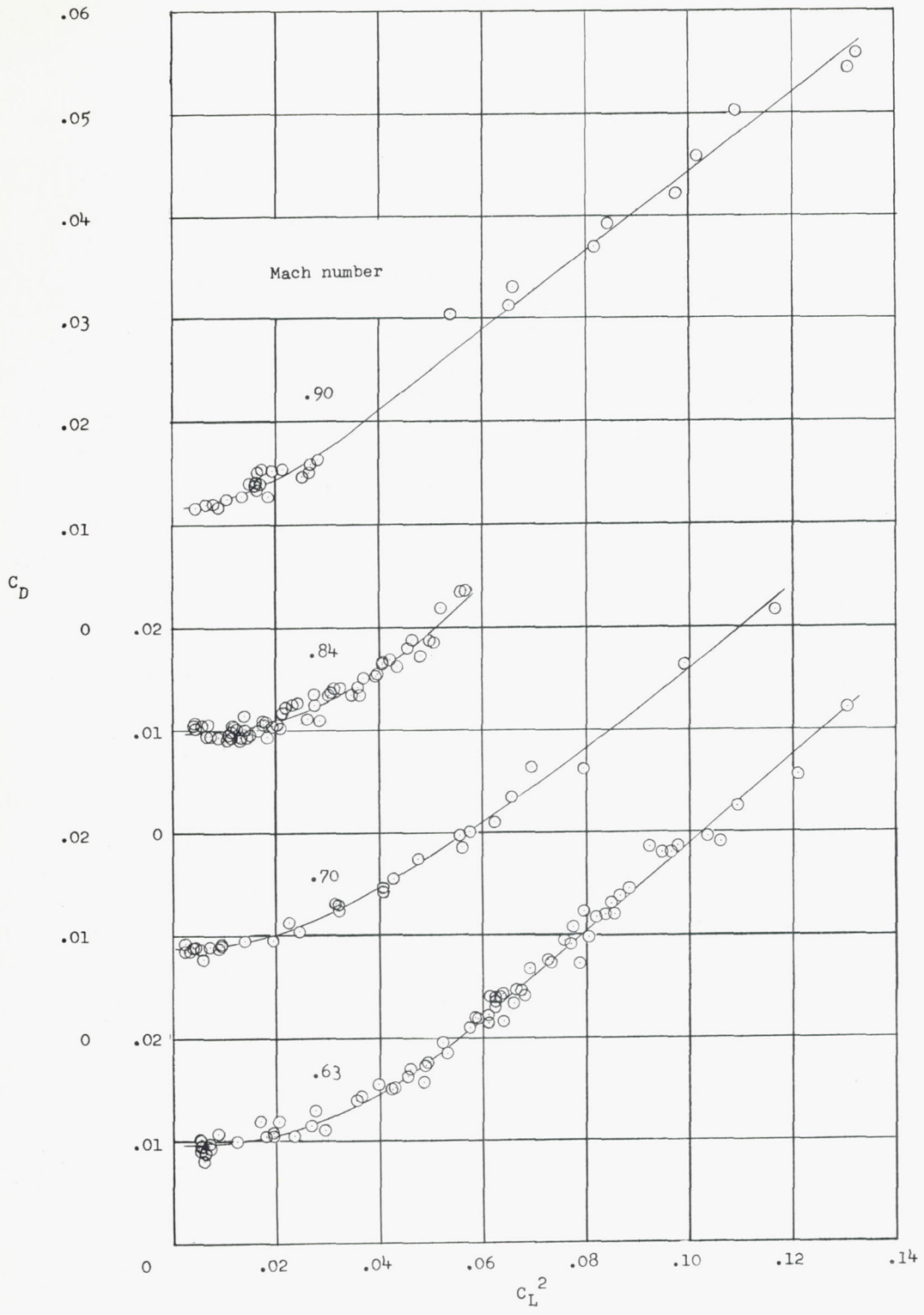

Figure 9.- Variation of drag coefficient with lift coefficient squared for four Mach numbers.